On the Origin of the Color in the Solid State. Crystal Structure and Optical and Magnetic Properties of 4-Cyanopyridinium Hydrogensquarate Monohydrate

Bojidarka B. Koleva,[†] Tsonko Kolev,*[,‡] Rüdiger W. Seidel,[†] Heike Mayer-Figge,[†] Michael Spiteller,[‡] and William S. Sheldrick[†]

Lehrstuhl für Analytische Chemie, Ruhr-Universität Bochum, Universitätsstrasse 150, 44780 Bochum, Germany, and Institut für Umweltforschung, Universität Dortmund, Otto-Hahn-Strasse 6, 44221 Dortmund, Germany

Received: November 10, 2007; In Final Form: January 8, 2008

The novel hydrogensquarate salt of 4-cyanopyridine was synthesized, and its structure and properties were elucidated in detail spectroscopically, thermally, and structurally, using single-crystal X-ray diffraction, linear-polarized solid-state IR spectroscopy, UV spectroscopy, TGA, DSC, DTA, and positive and negative ESI MS as well as ^{1}H and ^{13}C NMR methods. Quantum chemical methods were used to calculate the electronic structure, vibrational data, and electronic spectra. 4-Cyanopyridinium hydrogensquarate monohydrate crystallizes in the space group $P\bar{1}$ and exhibits a layered structure with molecules linked by intermolecular NH···$O_{(HSq-)}$ (2.651 Å) and HOH···$O_{(HSq^-)}$ (2.792 and 2.563 Å) hydrogen bonds with participation of cations, anions, and the solvent molecule. The formation of stable layers of the type $(2HSq^{-}.2H_2O)_n$ and the observation of a red color in the solid state is discussed. The optical and magnetic properties were elucidated in comparison to the data for neutral 4-cyanopyridine as well as its four known salts.

1. Introduction

As a part of our systematic investigation of aminopyridines, their metal complexes, and salts,[1−7] the spectroscopic and structural study of 4-cyanopyridinium hydrogensquarate monohydrate (Scheme 1) was performed. The crystal structure and optical and magnetic properties in solution and in the solid state were elucidated, using the methods of single-crystal X-ray diffraction, ^{1}H and ^{13}C NMR, positive and negative ESI mass spectrometry, UV spectroscopy, conventional and linear polarized IR spectroscopy, and TGV and DSC methods. Quantum chemical calculations at the DFT, MP2, and CIS levels of theory and a 6-311++G** basis set were employed for predicting and supporting the experimentally observed optical properties of the studied compound. Surprisingly, the compound possesses an intensive red color in the solid state, which is not typical for 4-cyanopyridinium salts. To date, only four crystallographic studies on this compound[8−11] have been reported in the literature in addition to the neutral compound.[12] Moreover, this phenomenon is unusual for other 2- and 3-cyanopyridinium salts and hydrogensquarates as well, which poses the question as to the origin of the color in the solid state for the present system. It is important to note, in this respect, that the investigated system is not a classical example of the crystallochromy effect, as studied in depth previously.[13−17]

2. Experimental Procedures

2.1. Methods. 2-, 3-, and 4-Cyanopyridines were purchased from Merck.

The X-ray diffraction intensities were measured in the ω scan mode on a Siemens P4 diffractometer equipped with Mo Kα radiation ($\lambda = 0.71073$ Å and $\theta_{max} = 25°$). The single-crystal X-ray diffraction data were corrected semiempirically for absorption, and the structure was solved by direct methods and refined against F^2.[18,19] An ORTEP plot illustrates the anion and cation structures at the 50% probability level. Relevant crystallographic structure data and refinement details are presented in Table 1, and selected bond distances and angles are presented in Table 2.

Conventional and polarized IR spectra were measured on a Thermo Nicolet OMNIC FTIR spectrometer (4000−400 cm^{-1}, 2 cm^{-1} resolution, and 200 scans) equipped with a Specac wire-grid polarizer. Nonpolarized solid-state IR spectra were recorded

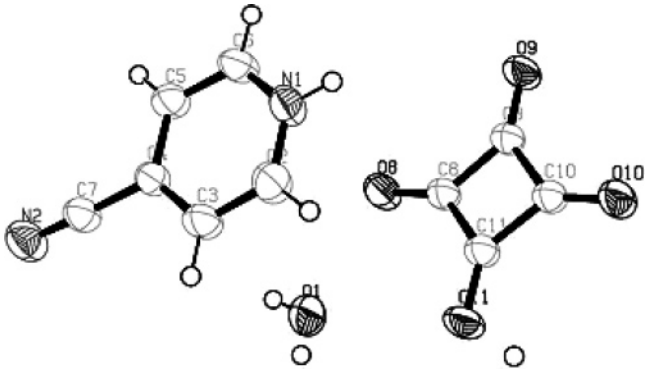

Figure 1. Molecular structure of 4-cyanopyridinium hydrogensquarate monohydrate, showing the atom-labeling scheme. Displacement ellipsoids are drawn at the 50% probability level.

SCHEME 1: Chemical Diagram of Compounds Studied

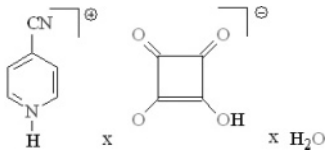

* Corresponding author. Tel.: ++49 0231 755 6970; e-mail: T.Kolev@infu.uni-dortmund.de.
[†] Ruhr-Universität Bochum.
[‡] Universität Dortmund.

10.1021/jp710765v CCC: $40.75
Published on Web 02/19/2008

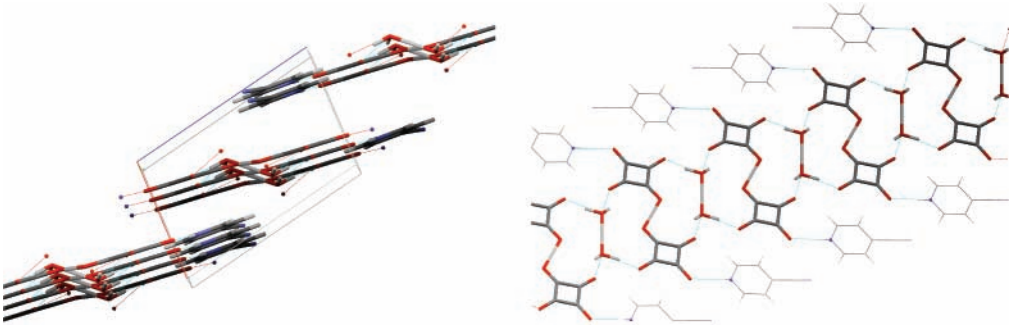

Figure 2. Linkage of the molecules of 4-cyanopyridinium hydrogensquarate monohydrate into infinite layers; stable layers of the repeated $2HSq^{-}\cdot 2H_2O$ fragment.

TABLE 1: Crystal Data and Data Collection and Refinement Conditions for 4-Cyanopyridinium Hydrogensquarate Monohydrate

empirical formula	$C_{10}H_8N_2O_5$
fw	236.18
temp (K)	294(2)
wavelength (Å)	0.71073
cryst syst, space group	triclinic, $P\bar{1}$
unit cell dimensions	$a = 6.7294(6)$ Å, $b = 7.934(3)$ Å, $c = 10.2031(11)$ Å $\alpha = 98.531(15)°$, $\beta = 97.238(8)°$, $\gamma = 106.844(13)°$
vol (Å^3)	507.3(2)
Z	2
calcd density (mg/m^3)	1.546
abs coeff (mm^{-1})	0.127
$F(000)$	244
cryst size	0.59 mm × 0.44 mm × 0.44 mm
θ range for data collection (deg)	2.73−24.98
limiting indices	$-1 \le h \le 7$, $-9 \le k \le 9$, $-12 \le l \le 12$
absorption correction	semiempirical
refinement method	full-matrix least-squares on F^2
reflns collected/unique	2207/1734 [R(int) = 0.0159]
data/restraints/params	1734/3/163
goodness-of-fit on F^2	1.057
final R indices [$I > 2\sigma(I)$]	$R1 = 0.0368$, wR2 = 0.0975
R indices (all data)	$R1 = 0.0445$, wR2 = 0.1036

TABLE 2: Selected Bond Lengths and Angles for 4-Cyanopyridinium Hydrogensquarate Monohydrate

N1−C2	1.327(2)	O8−C8	1.263(2)
N1−C6	1.334(2)	O9−C9	1.2469(18)
N2−C7	1.136(2)	O10−C10	1.317(19)
C2−C3	1.371(2)	O11−C11	1.2778(18)
C3−C4	1.377(2)	C8−C11	1.436(2)
C4−C5	1.385(2)	C8−C9	1.456(2)
C4−C7	1.444(2)	C9−C10	1.481(2)
C5−C6	1.362(2)	C10−C11	1.455(2)
C2−N1−C6	122.16(14)	C11−C8−C9	90.68(13)
N1−C2−C3	120.72(15)	O9−C9−C8	134.96(14)
C2−C3−C4	117.98(15)	O9−C9−C10	135.76(14)
C3−C4−C5	120.42(15)	C8−C9−C10	89.26(12)
C3−C4−C7	120.49(14)	O10−C10−C11	136.09(14)
C5−C4−C7	119.08(14)	O10−C10−C9	134.94(14)
C6−C5−C4	118.76(15)	C11−C10−C9	88.96(12)
N1−C6−C5	119.96(15)	O11−C11−C8	133.30(14)
N2−C7−C4	178.17(18)	O11−C11−C10	135.61(14)
O8−C8−C11	135.85(14)	C8−C11−C10	91.09(12)
O8−C8−C9	133.47(14)		

using the KBr disk technique. The oriented samples were obtained as a colloid suspension in a nematic liquid crystal ZLI 1695. The theoretical approach, as well as the experimental technique for preparing the samples and procedures for polarized IR spectral interpretation and the validation of this new linear-dichroic infrared (IR-LD) orientation solid-state method for accuracy and precision, has been presented previously. The influence of the liquid crystal medium on peak positions and integral absorbances of the guest molecule bands, the rheological model, the nature and balance of the forces in the nematic liquid crystal suspension system, and the morphology of the suspended particles also have been discussed.[20−23] 4CNPy also can be studied in a classical manner as an oriented film following cooling of the melted sample.

The positive and negative ESI mass spectra were recorded on a Finnigan LCQ instrument. UV spectra were recorded on a Tecan Safire Absorbance/Fluorescence XFluor 4 V 4.40 spectrophotometer operating between 190 and 900 nm, both in solid state and in solution at a concentration of 2.5×10^{-5} M, using 0.0921 cm quarz cells.

Quantum chemical calculations were performed with the Gaussian 98 program packages.[24] The output files were visualized by means of the ChemCraft program.[25] The geometries of neutral and protonated forms of 4CNPy were optimized at two levels of theory: second-order Møller−Plesset perturbation theory (MP2) and density functional theory (DFT) using the 6-311++G** basis set. The DFT method employed was B3LYP, which combines Becke's three-parameter nonlocal exchange function with the correlation function of Lee, Yang, and Parr. Molecular geometries of the studied species were fully optimized by the force gradient method using Berny's algorithm. For every structure, the stationary points found on the molecule potential energy hypersurfaces were characterized using standard analytical harmonic vibrational analysis. The absence of the imaginary frequencies, as well as of negative eigenvalues of the second-derivative matrix, confirmed that the stationary points correspond to minima of the potential energy hypersurfaces. The calculated vibrational frequencies and infrared intensities were checked to establish as to which kind of performed calculations agreed best with the experimental data. In our case, the DFT method provided more accurate vibrational data, as far as the calculated standard deviations of, respectively, 8 cm^{-1} (B3LYP) and 13 cm^{-1} (MP2) are concerned, which correspond to groups not participating in significant intra- or intermolecular interactions. The B3LYP/6-311++G** data are presented for the previously discussed modes, where a modification of the results using an empirical scaling factor of 0.9614 was made to achieve better correspondence between the experimental and the theoretical values. The UV spectra of the compound in the gas phase and in the ethanol solution were obtained by CIS/6-311++G** and TD DFT calculations.

Thermal analyses were performed in the 300−500 K region on a PerkinElmer DSC-7 differential scanning calorimeter and a differential thermal analyzer (DTA/TG) (Seiko Instruments, model TG/DTA 300). The experiments were carried out at a scanning rate of 10 K/min under an argon atmosphere. The

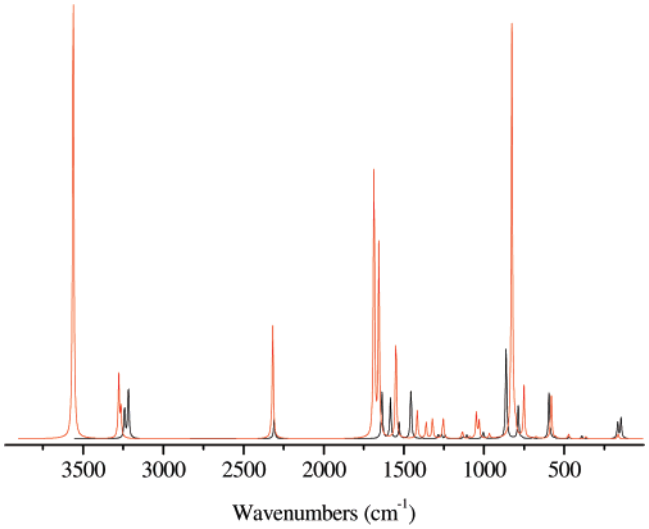

Figure 3. Theoretical IR spectra of 4CNPy (black line) and its N_{py} protonated form (red line).

elemental analysis was carried out according to the standard procedures for C and H (as CO_2 and H_2O) and N (by the Dumas method).

2.2. Synthesis. 4-Cyanopyridinium hydrogensquarate monohydrate was synthesized by mixing equimolar amounts of 4-cyanopyridine (0.3214 g) and squaric acid (0.1141 g) dissolved in 5 mL of water with continuous stirring and heating at 100 °C for 6 h. After 1 week, red crystals were obtained from the resulting yellow solution and were filtered off and dried under air. (Found: C, 50.87; H, 3.10; N, 11.88%; $[C_{10}H_8N_2O_5]$ calcd: C, 50.85; H, 3.41; N, 11.86%). The most intensive signal in the positive ESI mass spectrum was that of the peak at *m*/*z* 105.22, corresponding to the singly charged cation $[C_6H_5N_2]^+$ with a molecular weight of 105.12. The negative ESI mass spectrum showed a peak at *m*/*z* 113.40 corresponding to the singly charged $[C_4HO_4]^-$ anion with a molecular weight of 113.05. The TGV and DSC data in the temperature range of 300−500 K illustrated a molecular weight loss of 7.66% and an enthalpy effect of 3.16 kcal/mol at 399 K, corresponding to loss of the water molecule included in the crystal structure of the newly synthesized compound. During this process, a change in color from red to colorless was observed for the resulting amorphous sample.

3. Results and Discussion

3.1. Crystal Structure. 4-Cyanopyridnium hydrogensquarate monohydrate crystallizes in the space group *P*1 (Figure 1). The molecules are joined together (Figure 2) by moderately strong intermolecular $NH\cdots O_{(HSq^-)}$ (2.651 Å) and $HOH\cdots O_{(HSq^-)}$ (2.792 and 2.563 Å) hydrogen bonds with the participation of cations, anions, and the solvent molecule. This led to the presence of $(2HSq^-.2H_2O)_n$ layers (Figure 2). The hydrogensquarate (HSq^-) anions form stable dimers with a proton disordered equally between the anions. The molecule of the cation is flat with a maximal deviation from total planarity of less than 0.2° and with bond lengths and angles (Table 2) that are typical in comparison to the data for the four known salts of 4CNPy.[8-11]

3.2. Theoretical and Experimental IR Spectroscopic Data. Calculated IR spectra of neutral and N_{py} protonated 4-cyanopyridine are shown in Figure 3. Excluding the observation of the new typical IR bands of the NH^+ group (ν_{NH_+} stretching

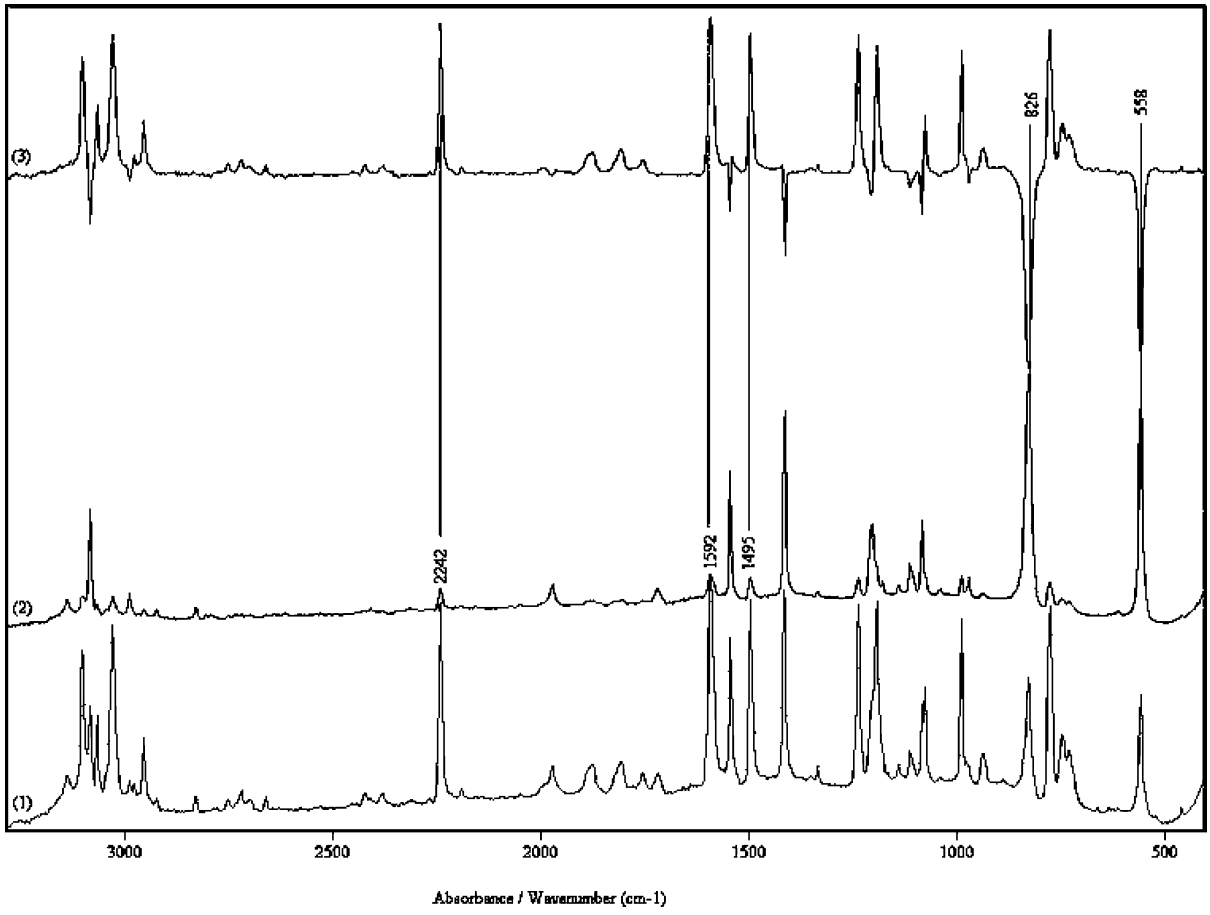

Figure 4. Parallel (1), perpendicular (2), and difference (3) IR-LD spectra of 4CNPy.

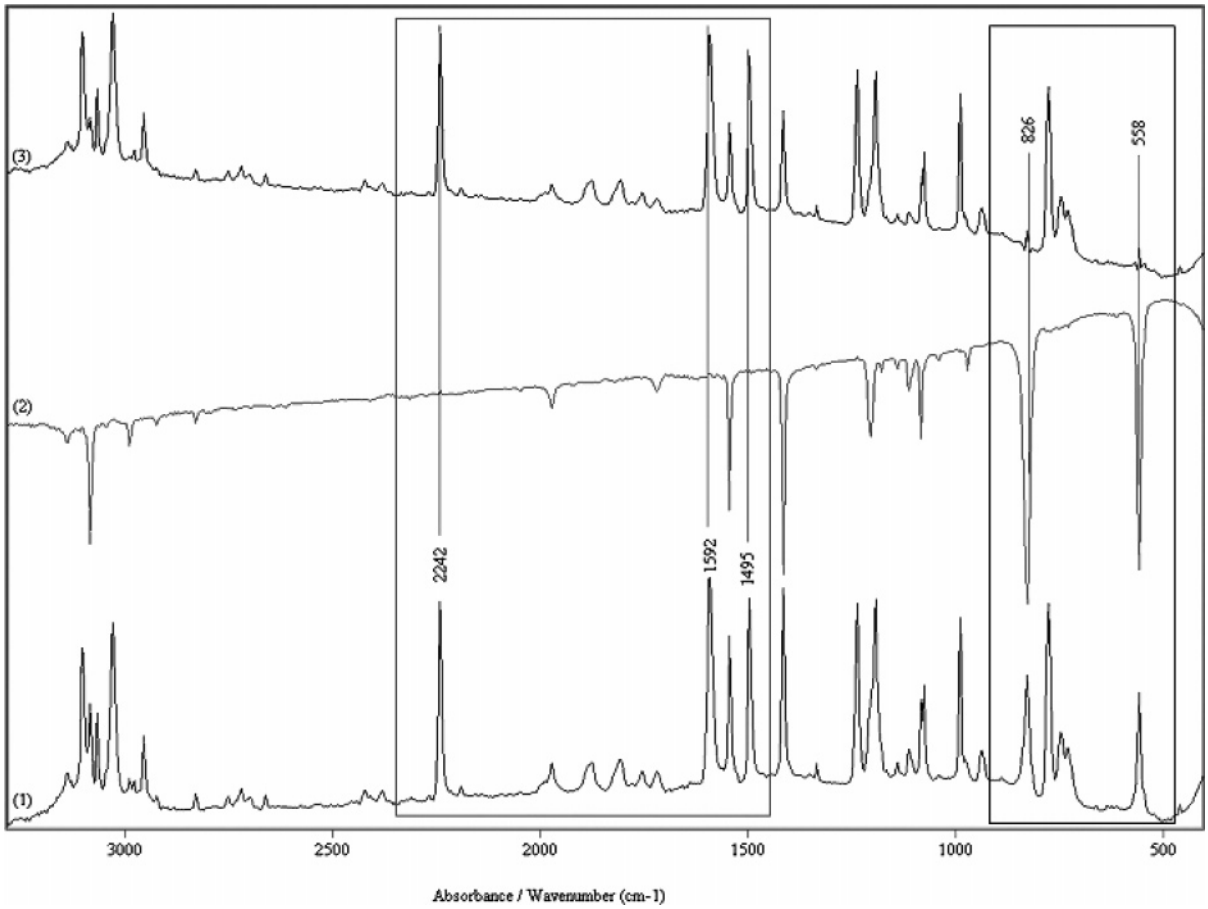

Figure 5. Nonpolarized IR (1) and reduced IR-LD spectra of 4CNPy after elimination of the bands at 1592 cm^{-1} (2) and 826 cm^{-1} (3).

SCHEME 2: Illustration of Some Transition Moments of N_{py} Protonated 4CNPy

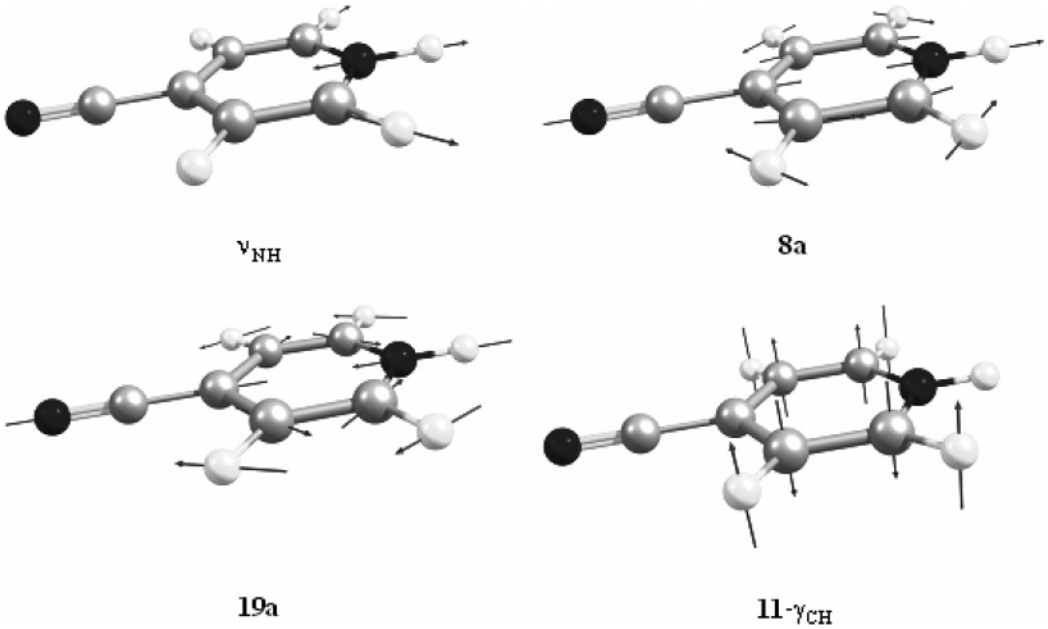

and δ_{H_+} banging modes) at 3424 and 1592 cm^{-1}, the characteristic IR bands of the pyridinium ring and the substituent CN group were hardly affected by the N_{py} protonation. The ν_{CN} frequency was shifted to the higher wavenumbers by 4 cm^{-1} following protonation and was predicted to be 2228 cm^{-1} (Scheme 2). An increase in intensity and a high-frequency shifting of the in-plane aromatic bands in the 1700−1500 cm^{-1} region of less than 5 cm^{-1} were calculated for the N_{py} protonated form (bands at 1620 and 1491 cm^{-1} in Scheme 2). This was also the case for the out-of-plane band (B_1) **11**-γCH at 820 cm^{-1} (Scheme 2).

The polarized IR-LD spectra of 4CNPy (Figure 4) show a significant degree of macro-orientation of the sample[20−23] along the *c*-crystallographic axis. As can be seen, the difference IR-LD spectrum (Figure 4, spectrum 3) is characterized by positive absorption bands at 1592 and 1495 cm^{-1} corresponding to **8a**

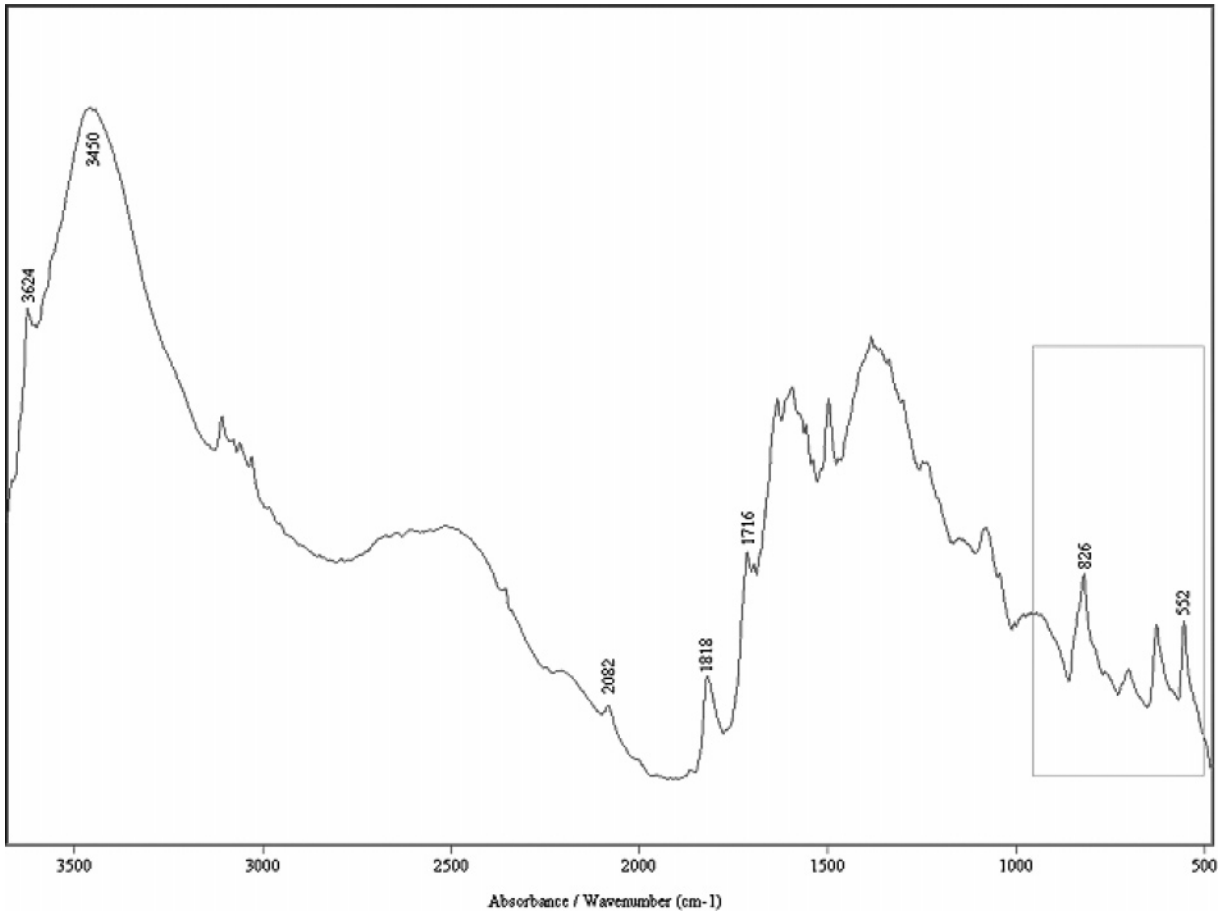

Figure 6. IR spectrum of 4-cyanopyridinium hydrogensquarate monohydrate.

SCHEME 3: Unit Cell of 4CNPy[12]

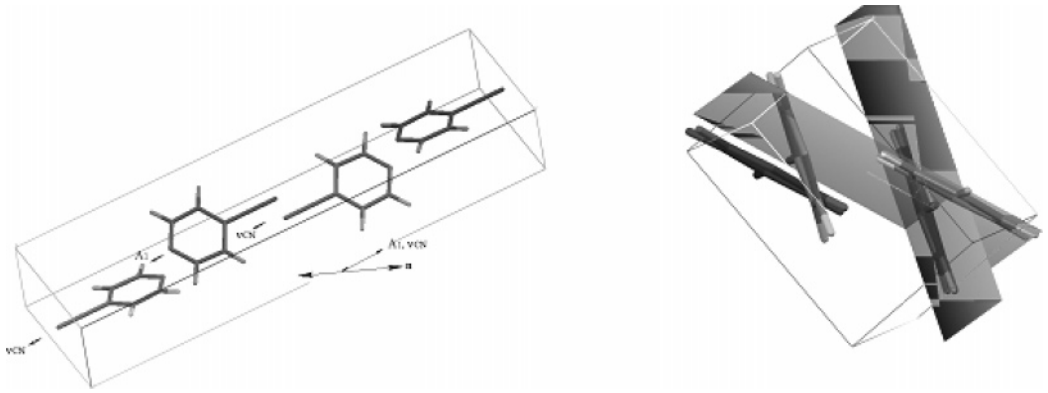

and **19a** in-plane modes, with transition moments along the C−CN band (Scheme 3). For the same reason, the positive ν_{CN} stretching mode at 2242 cm^{-1} is expected. Within the unit cell of neutral 4CNPy,[12] all of the molecules are oriented in the same way (Scheme 3), which causes a collinear orientation of the discussed transition moments. The elimination of these bands at an equal dichroic ratio (Figure 5, spectrum 2) leads to full disappearance of each of the bands. In contrast, the elimination (Figure 5, spectrum 3) of the out-of-plane modes at 826 cm^{-1} (**11**-γ_{CH}) and 558 cm^{-1} (γ_{CN}) leads to observation of second neighboring peaks, due to the planes of the pyridinium rings adopting an angle of 43.3(5)° in the unit cell (Scheme 3). A comparison of the data of neutral 4CNPy with the characteristic IR bands of the studied hydrogensquarate salt (Figure 6) points to strong overlapping and an underlined Evans hole effect in the second case. This state of affairs is typical for systems with infinite layer structures and strong hydrogen bonding. The highest absorption bands at 3624 and 3450 cm^{-1} correspond to ν_{OH} of the free and bonded solvent molecules. The whole 3300−2080 cm^{-1} region is attributed to ν_{OH} vibrations of HSq^- fragments involved in strong intermolecular hydrogen bonding. This band overlaps with the ν_{NH^+} stretching vibration, which prevents its experimental assignment. The bands at 1818 and 1716 cm^{-1} belong to $\nu^{s}_{C=O}$ and $\nu^{as}_{C=O}$ of the latter moieties. The out-of-plane bands that are characteristic for 4CNPy can be observed in the salt as well, thereby confirming that N_{py} protonation does not significantly affect the aromatic character of the pyridinium system, as is typical for 4-aminopyridinium salts [2,6]. Looking at the IR pattern of the hydrogensquarate salt of 4-cyanopyridinium, the strong mutual interaction of the

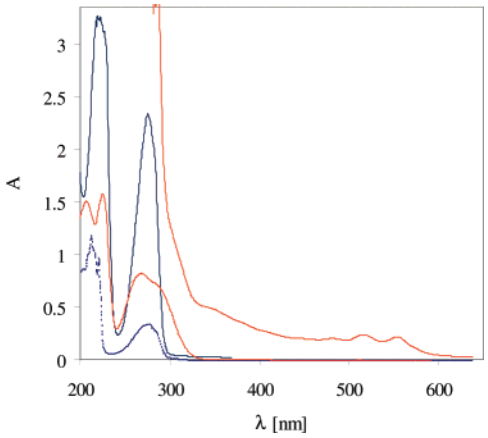

Figure 7. UV spectra of 4CNPy (dotted blue line) and its hydrogensquarate (blue line) in 2.5×10^{-5} M water solution; solid-state UV spectra of 4-cyanopyridnium hydrogensquarate monohydrate (red lines).

HSq^- and H_2O molecules leads to the observation of intensive broad bands with the predominant character of their characteristic IR bands. This observation is independent of the theoretically predicted stronger increases in intensity for some of the characteristic IR bands of the N_{py} protonated 4CNPy cation. The strong Evans hole effect leads here to a rise in the spectral curve. This phenomenon combined with the extremely low-frequency shifting of the $\nu_{OH(Sq)}$ sub maximum up to 2080 cm^{-1} suggests that we can describe the system as consisting of infinite layers of repeated strongly interacting $2HSq^-.2H_2O$ fragments, where the cation only has the function to stabilize the layers. This assumption is in accordance with the electronic spectrum of the compound, where a significant bathochromic effect of the charge-transfer (CT) band is observed in the solid state.

3.3. UV−Vis Spectra. The UV spectra of 4CNPy and its hydrogensquarate in H_2O solution are depicted in Figure 7 and are characterized by bands at about 270 cm^{-1} (ϵ about 12 000 L mol^{-1} cm^{-1}) and 285 cm^{-1} (ϵ about 400 L mol^{-1} cm^{-1}), corresponding to the B-band of the pyridine fragment and to $n \rightarrow \pi$ transfer of the -CN substituent. In the case of the hydrogensquarate salt in solution, these bands overlap with the $n \rightarrow \pi$ bands of the HSq^- anions. These observed data correlate well with our theoretical calculations, where the bands at 266 nm ($f = 0.7821$) and 270 nm ($f = 0.9231$) are typical for the neutral and N_{py} protonated forms of 4CNPy. However, in the solid-state spectrum (Figure 7), two new bands at 530 and 570 nm with ϵ values of about 300 and 500 L mol^{-1} cm^{-1} are observed in the visible region. These bands are only observed for the 4-cyanopyridinium salts studied here and are absent in other cyanopyridinium salts previously reported.[8−11] These bands are responsible for the red color of the compound in the solid state. How can this phenomenon be explained? In comparison with the rare studies on crystallochromy, it is apparent that our system does not correspond to classical cases.[13−17] Looking to the crystal structure, we can propose that the red color is a result of a CT band within the layers formed by repeated $2HSq^-{\cdot}2H_2O$ fragments (Figure 2). Additional confirmation follows from the fact that the visible maxima disappear after the sample is heated to 120 °C, when the included solvent is evaporated (see TGV and DSC data).

3.4. ^{1}H and ^{13}C NMR Data in Solution. The ^{1}H NMR spectrum of the compound exhibits aromatic proton resonances of 4CNPy at 7.88 and 7.72 ppm, respectively. In comparison with the proton signals of the protonated hydrogensquarate salt, the chemical shift differences are less than 0.10 ppm. These data are in accordance with reported theoretical studies,[2,6] where it has been shown that Npy protonation only has a weak affect on the aromatic character of the pyridinum ring[2,6,7] in various cyano-substituted pyridines.

4. Conclusion

The crystal structure and optical and magnetic properties of the newly synthesized 4-cyanopyridinium hydrogensquarate monohydrate were elucidated in detail, using single-crystal X-ray diffraction, linear-polarized solid-state IR spectroscopy, UV−vis spectroscopy, TGA, DSC, DTA, and positive and negative ESI MS as well as ^{1}H and ^{13}C NMR methods. Quantum chemical calculations were used to obtain the electronic structure, vibrational data, and electronic spectra. 4-Cyanopyridinium hydrogensquarate monohydrate crystallizes in the space group $P\bar{1}$ and exhibits a layered structure with molecules linked by intermolecular $NH{\cdots}O_{(HSq-)}$ (2.651 Å) and $HOH{\cdots}O_{(HSq-)}$ (2.792 and 2.563 Å) hydrogen bonds with the participation of cations, anions, and the solvent molecule. The unusual red color of the compound in the solid state is proposed to be a result of a strong bathochromic shift of the CT band within the stable layers formed by the ($2HSq^-.2H_2O$) fragments.

Acknowledgment. B.B.K. thanks the Alexander von Humboldt Foundation for a fellowship, and T.K. thanks the DAAD for a grant within the priority program "Stability Pact South-Eastern Europe" and the Alexander von Humboldt Foundation. Crystallographic data for structural analysis have been deposited with the Cambridge Crystallographic Data Centre, CCDC 666862. Copies of this information may be obtained from the Director, CCDC, 12 Union Road, Cambridge, CB2 1EZ, U.K. (fax: +44 1223 336 033; e-mail: deposit@ccdc.cam.ac.uk or http://www.ccdc.cam.ac.uk).

References and Notes

(1) Ivanova, B. B.; Mayer-Figge, H. *J. Coord. Chem.* **2005**, *58*, 653.
(2) Ivanova, B. B.; Arnaudov, M. G.; Mayer-Figge, H. *Polyhedron* **2005**, *24*, 1624.
(3) Koleva, B. B.; Trendafilova, E. N.; Arnaudov, M. G.; Sheldrick, W. S.; Mayer-Figge, H. *Transition Met. Chem. (Dordrecht, Neth.)* **2006**, *31*, 866.
(4) Kolev, T.; Koleva, B. B.; Spassov, T.; Cherneva, E.; Spiteller, M.; Sheldrick, W. S.; Mayer-Figge, H. *J. Mol. Struct.* **2007**, in press.
(5) Koleva, B. B.; Tsanev, T.; Kolev, T.; Mayer-Figge, H.; Sheldrick, W. S. *Acta Crystallogr., Sect. E: Struct. Rep. Online* **2007**, in press.
(6) Koleva, B. B.; Kolev, T.; Tsanev, T.; Kotov, S.; Mayer-Figge, H.; Seidel, R. W.; Sheldrick, W. S. *J. Mol. Struct.* **2007**, in press.
(7) Koleva, B. B.; Kolev, T.; Tsanev, T.; Kotov, S.; Mayer-Figge, H.; Seidel, R. W.; Sheldrick, W. S. *Struct. Chem.* **2007**, in press.
(8) Smith, G.; Wermuth, U. D.; Healy, P. C.; White, J. M. *Aust. J. Chem.* **2003**, *56*, 707.
(9) Ren, P.; Qin, J.; Liu, T.; Zhang, S. *Inorg. Chem. Commun.* **2004**, *7*, 134.
(10) Dega-Szafran, Z.; Gdaniec, M.; Grundwald-Wyspianska, M.; Kosturkiewicz, Z.; Koput, J.; Krzyzanowski, P.; Szafran, M. *J. Mol. Struct.* **1992**, *270*, 99.
(11) Bailey, R. D.; Drake, G. W.; Grabarczyk, M.; Hanks, T. W.; Hook, L. L.; Pennington, W. T. *J. Chem. Soc., Perkin Trans. 2* **1997**, 2773.
(12) Laing, M.; Sparrow, N.; Sommerville, P. *Acta Crystallogr., Sect. B: Struct. Sci.* **1971**, *27*, 1986.
(13) Wang, Z.; Qi, Y.; Gao, J.; Sacripante, G.; Sundararajan, P.; Duff, J. *Macromolecules* **1998**, *31*, 2075.
(14) Aakeroy, C. B. *Acta Crystallogr., Sect. B: Struct. Sci.* **1997**, *53*, 569.
(15) El-Sayed, M.; Muller, H.; Rheinwald, G.; Lang, H.; Spange, S. *Chem. Mater.* **2003**, *15*, 746.
(16) Klebe, G.; Graser, F.; Kdicke, E.; Bernd, J. *Acta Crystallogr., Sect. B: Struct. Sci.* **1989**, *45*, 69.

(17) Kazmaiergt, P. M.; Hoffmannt, R. *J. Am. Chem. Soc.* **1994**, *116*, 9684.

(18) Sheldrick, G. M. *SHELXTL, Release 5.03 for Siemens R3 Crystallographic Research System*; Siemens Analytical X-Ray Instruments, Inc.: Madison, WI, 1995.

(19) Sheldrick, G. M. *SHELXS97 and SHELXL97*; University of Göttingen: Göttingen, Germany, 1997.

(20) Ivanova, B. B.; Arnaudov, M. G.; Bontchev, P. R. *Spectrochim. Acta, Part A* **2004**, *60*, 855.

(21) Ivanova, B. B.; Tsalev, D. L.; Arnaudov, M. G. *Talanta* **2006**, *69*, 822.

(22) Ivanova, B. B.; Simeonov, V. D.; Arnaudov, M. G.; Tsalev, D. L. *Spectrochim Acta, Part A* **2007**, *67*, 66.

(23) Koleva, B. B.; Kolev, T.; Simeonov, V.; Spassov, T.; Spiteller, M. *Colloids Surf.* **2007**, submitted.

(24) Frisch, M. J.; Trucks, G. W.; Schlegel, H. B.; Scuseria, G. E.; Robb, M. A.; Cheeseman, J. R.; Zakrzewski, V. G.; Montgomery, J. A., Jr.; Stratmann, R. E.; Burant, J. C.; Dapprich, S.; Millam, J. M.; Daniels, A. D.; Kudin, K. N.; Strain, M. C.; Farkas, Ö.; Tomasi, J.; Barone, V.; Cossi, M.; Cammi, R.; Mennucci, B.; Pomelli, C.; Adamo, C.; Clifford, S.; Ochterski, J.; Petersson, G. A.; Ayala, P. Y.; Cui, Q.; Morokuma, K.; Salvador, P.; Dannenberg, J. J.; Malick, D. K.; Rabuck, A. D.; Raghavachari, K.; Foresman, J. B.; Cioslowski, J.; Ortiz, J. V.; Baboul, A. G.; Stefanov, B. B.; Liu, G.; Liashenko, A.; Piskorz, P.; Komáromi, I.; Gomperts, R.; Martin, R. L.; Fox, D. J.; Keith, T.; Al-Laham, M. A.; Peng, C. Y.; Nanayakkara, A.; Challacombe, M.; Gill, P. M. W.; Johnson, B.; Chen, W.; Wong, M. W.; Andres, J. L.; Gonzalez, C.; Head-Gordon, M.; Replogle, E. S.; Pople, J. A. *Gaussian 98*; Gaussian, Inc.: Pittsburgh, PA, 1998.

(25) Zhurko, G. A.; Zhurko, D. A. *ChemCraft: Tool for Treatment of Chemical Data*; Lite Version Build 08 (freeware): 2005.